



Copyright © IJCESEN

*International Journal of Computational and
Experimental Science and Engineering*
(IJCESEN)

Vol. 3-No.2 (2017) pp. 20-25

<http://iakkurt.dergipark.gov.tr/ijcesen>



ISSN: 2149-9144

Research Article

A Computational Comparison of Flow and Pressure Fields in Axial and Reverse Flow Cyclone Separators

Ali SAKIN¹, İrfan KARAGÖZ^{2*}, Atakan AVCI²

¹ TOFAS-FIAT R&D Department, 16369, Bursa-Turkey

² Uludag University, Department of Mechanical Engineering, 16059, Bursa-Turkey

* Corresponding Author : karagoz@uludag.edu.tr

(First received 25 November 2016 and in final form 20 May 2017)

Presented in "3rd International Conference on Computational and Experimental Science and Engineering (ICCESEN-2016)"

Keywords

Two phase flow
Separation efficiency
Pressure drop
CFD

Abstract: Cyclones are separation devices that use centrifugal forces to remove dense phases from two phase flows. There are many application areas of cyclone separators ranging from industrial processes to domestic applications due to their simple structure and lack of movable components. For this reason, they are commonly preferred where two phase fluid flow accommodated and separation is required. In this study, axial and reverse flow tangential inlet novel cyclone geometries were introduced to configure different separation space and to reduce pressure drop in comparison with traditional cyclone geometry. Although the construction of a cyclone is simple, the cyclone flow and separation process are very complex. Therefore, CFD is quite appropriate provided that the proper mathematical models and computational techniques are used. 3-D and unsteady governing equations were used for the turbulent cyclone flow. Hexahedral meshed domain was solved by using Fluent CFD software. Eulerian approach was used to solve the flow field and transient Reynolds Stress Model (RSM) with the scalable wall function. Lagrangian approach with DPM (Discrete Phase Model) was used to calculate discrete phase by releasing particles from inlet surface. CFD calculations were run for different geometric configurations in order to analyze performance of cyclones in terms of pressure drop, cut-off diameter and grade efficiency. Axial and tangential velocity profiles are presented at defined sections. The computational results of pressure drop, velocity field and separation efficiency were also compared for the axial and reverse flow cyclones at the same flow rates.

1. Introduction

Cyclones are widely used in different industries where two phase fluid flow is accommodated. Cyclones are commonly used due to their simple structure, non-movable parts and low operation cost. In this study, axial and reverse flow tangential inlet novel cyclone geometries were introduced to configure different separation space and to reduce pressure drop in comparison with traditional cyclone geometry. Several empirical models have been proposed to explain and enhance cyclone performance [1]. According to Stern et al. [2] a cone is not an essential part of cyclone it was used for delivery of collected particles to central

discharge point. In contrary, Zhu and Lee [3] stated that conical part of the cyclone geometry provides greater tangential velocities at the bottom of the cyclone which is essentially important for particle removal. Recently Karagoz et al. [4] presented a novel reverse flow cyclone geometry and design of this cyclone is based on configuration of separation space and they investigated effect of vortex limiter on cyclone performance experimentally. Fuat et al. [5] studied effect of geometrical parameters (cone bottom and vortex finder diameter, cyclone length and inlet velocity). They found that pressure drop in the new cyclone are slightly higher than in the conventional cyclone under the same geometrical and operational conditions. Oh et al. [6] studied

uniflow cyclone concept and they stated that particle separation efficiency was increased with increasing length of the gas outlet tube at a certain value. For the greater tube length, particle separation efficiency decreases. In this study, axial and reverse flow tangential inlet novel cyclones were studied numerically. In contrary to reverse flow cyclone, vortex formation of axial flow cyclone develops differently due to bottom outflow condition.

2. NUMERICAL MODELLING

2.1 Axial and Reverse Flow Cyclones Geometrical Configurations

Two types of cyclone flow were studied in scope of this work. Axial and reverse flow cyclone geometries are shown in Figure 1(a-c) and characteristic are given in Table 1.

Table 1. Separator dimensions (unit: mm)

a	inlet height	74
b	inlet width	16
D	body diameter	150
D₁	cyclone diameter	80
D₂	vortex finder / outlet diameter	30
s	vortex finder length	80

For the axial flow cyclone geometry, L_b represents the start of exit tube instead of vortex limiter position. Numerical analyses of axial and reverse flow novel cyclone geometries were run for

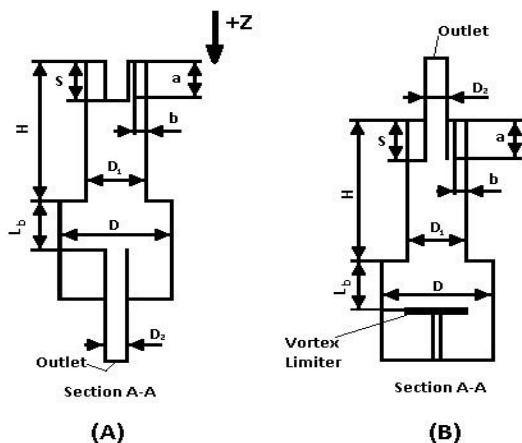


Figure 1. Axial flow cyclone geometry (a), reverse flow cyclone geometry (b), top view of cyclones (c) ANSYS ICEM CFD V15 software was used to create numerical domain and hexahedral mesh

different configurations of surface friction height and vortex limiter position as shown in Table 2.

Table 2. Separator configurations (unit: mm)

H (Surface Friction Length)	L_b (Vortex Limiter Position)			
	290	100	400	600
435	100	300	400	
580	100	200		

2.2 Numerical Method

Eulerian-Lagrangian approach was used for numerical calculations of gas-solid flow in this study and flow was assumed as unsteady, incompressible and turbulent. Continuity and momentum equations were solved in order to obtain velocity field. The turbulent flow was represented by Reynolds Stress Model (RSM) and particle trajectories and collection efficiencies were calculated by Lagrangian approach. Numerous particles which were injected from inlet surface were followed through the flow field by solving the particle force balance equation of motion. Flow field was defined as three dimensional. The volume fraction of the dispersed phase did not exceed 10 %, so particle-particle interaction can be neglected and particle phase did not affect flow field. Therefore problem was assumed as one way coupling [8]. Numerical domain was created for all type of geometries are given in Table 2 for both axial and reverse flow cyclones. structure was employed for all solutions. Mesh sensitivity analyses were performed and trial numerical results demonstrated that most efficient grid numbers for axial and reverse flow cyclones varied between 125.000-346.000 and 260.000 to 535.000 respectively. A common CFD commercial code ANSYS Fluent V15 was used for calculation of numerical domain. Kaya and Karagoz [7] analyzed various numerical schemes for swirl dominated flows and the most appropriate numerical schemes are given in Table 3.

2.3 Boundary Conditions and Other Settings

CFD analysis was begun with steady state lower order numerical schemes and then switched to

Table 3. Numerical schemes

Pressure Coupling	Velocity	SIMPLEC
-------------------	----------	---------

Pressure Interpolation	PRESTO
Momentum	QUICK
Turbulent Kinetic Energy	2 nd Order Upwind
Dissipation Rate	2 nd Order Upwind
Reynolds Stresses	1 st Order Upwind

transient higher order schemes in order to overcome convergence difficulties. Scalable wall functions were employed for near wall treatment to avoid deterioration of standard wall functions under a grid refinement below $y^+ < 11$ [10]. These wall functions produce consistent results for grids of arbitrary refinement. For grids that are coarser than $y^+ > 11$, the standard wall functions are identical. Velocity inlet boundary condition was applied at inlet, outflow at gas exit and wall (no-slip) condition at other boundaries. Volumetric flow rate equals to 55 m³/h, dynamic viscosity of 2.11E-5 Pa s and air density 1.0 kg/m³. The turbulence intensity and the hydraulic diameter were defined as 5 % and 0.0263 m respectively. Density of released particle is 2700 kg/m³ and maximum time steps number was 10E5 steps for each injection. Time step per iteration was taken as 0.0001 s.

3 Results

Comparison of axial and reverse flow novel cyclones were carried out for different geometrical conditions explained in Table 2. Pressure drop and cut-off diameter results were presented for all configurations. Further explanations were made by using surface friction length of 290 mm for both axial and reverse flow novel cyclones in order to prevent exceeding page number.

3.1 Pressure Drop

Pressure drop values of axial and reverse flow novel cyclone are given in Figure 2. For the axial flow novel cyclone, pressure drop decreases with increased vortex limiter position and surface friction length. Pressure drop trend was same for reverse flow novel cyclone but pressure drop change of geometrical configurations was not significant as axial flow. For the further explanation, surface friction length (H) of 290 mm was chosen and flow field variables were plotted at the half height of the vortex limiter position for all geometric configurations. Axial and tangential velocity profiles of H=290 mm are given in Figure 4 and 5.

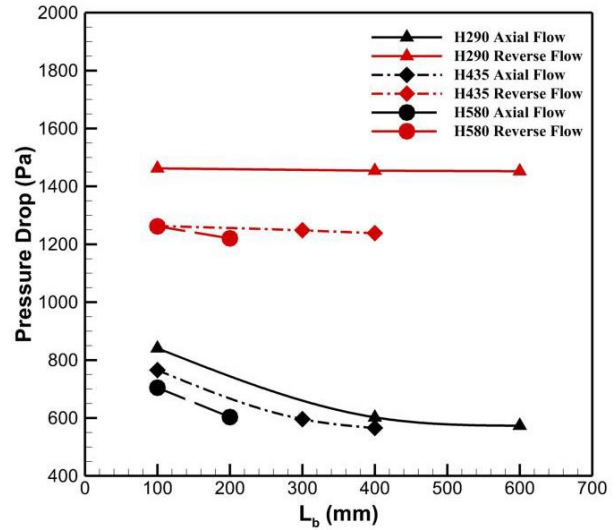


Figure 2. Pressure drop values of different geometric configurations for axial and reverse flow novel cyclones

From Figure 2, It can be clearly seen that pressure drop decreases with increase in surface friction length (H). This can be explained by tangential velocity profiles because tangential velocity is the major component that affects pressure drop. Figure 3 illustrates that tangential velocity is decreasing with increase in surface friction length and consequently pressure drop decreases. Similarly pressure drop decreases with increasing vortex limiter position and Figure 3 and 4 represents tangential and axial velocity profile for different vortex limiter positions (L_b) at constant surface friction length (H). According to Figure 4, tangential velocity is maximum for the smallest surface friction length (H) so pressure drop is greater than other configurations due to surface friction. Similarly, increasing vortex limiter position (L_b) causes weaker swirl and tangential velocity decreases in parallel with pressure drop is decreased. Axial flow cyclones have smaller pressure drop according to reverse flow cyclones. Vortex formation of axial flow cyclones is more different than reverse flow and there is no energy loss between downward and upward flow in terms axial velocity so axial flow cyclones have less dissipation losses according to reverse flow. In Figure 5, at defined section there is no upward flow for axial flow cyclones. For the reverse flow novel cyclones, EOVC occurred for all configurations and vortex end bends to the wall instead of centralized vortex formation (Figure 6). Pressure drop is not significantly affected by vortex limiter position due to EOVC at constant surface friction length. EOVC was not occurred

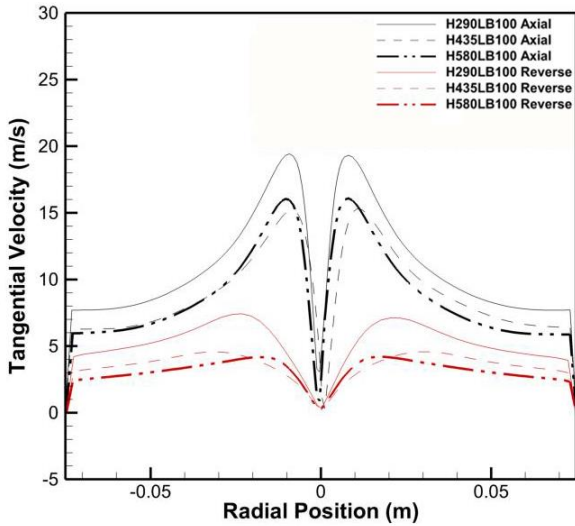


Figure 3. Tangential velocity profiles of $LB = 100$ mm for axial and reverse flow novel cyclones at $z = H + (L_b/2)$

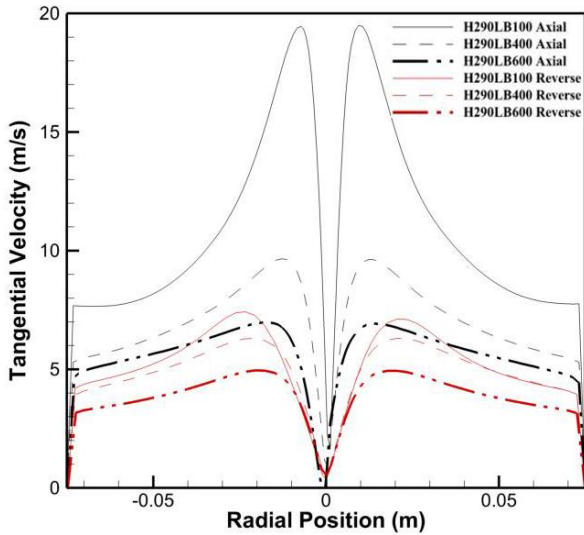


Figure 4. Tangential velocity profiles of $H = 290$ mm for axial and reverse flow novel cyclones at $z = H + (L_b/2)$

for axial flow novel cyclones due to nature of direction of flow and lack of reverse flow (Figure 6) so pressure drop is less as expected.

3.1 Collection Efficiency

Collection efficiency of axial and reverse flow novel cyclones is given in Figure 7. For Axial flow novel cyclones, collection efficiency decreases with increasing vortex limiter position (L_b) and surface friction length (H) due to weaker tangential velocity profile and swirl as explained previously. For reverse flow cyclone configurations, particle collection efficiency is decreased with increasing surface friction length (H) similarly as axial flow cyclones. Particle collection efficiency is decreased

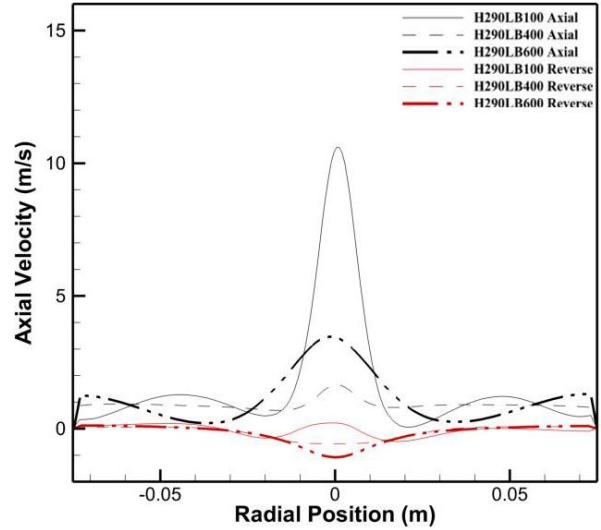


Figure 5. Axial velocity profiles of $H = 290$ mm for axial and reverse flow novel cyclones at $z = H + (L_b/2)$

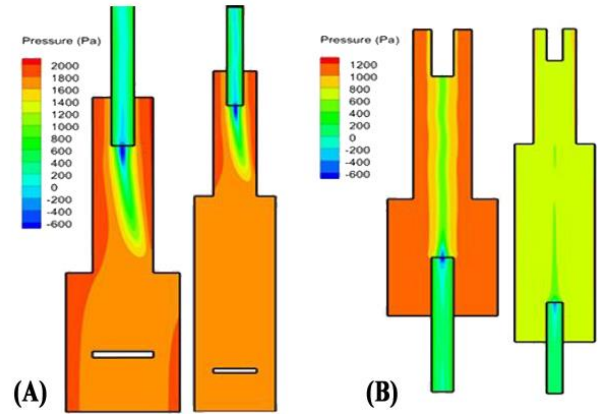


Figure 6. Static pressure contours of reverse flow of H290LB100 and LB400 (A), axial flow of H290LB100 and LB400 (B)

with increase in vortex limiter position except $H = 580$ mm and change of efficiency is not significant as axial flow cyclones.

Contrary to axial flow, cut-off diameter of reverse flow cyclone is not changing significantly for same frictional surface length (H) due to EOVS. Below the vortex end, separation efficiency depends on induced secondary vortex, just downstream of it due to fluid coupling. It should be stated that induced vortex of $H = 580$ mm is more effective in separation space. Furthermore particle collection efficiency is improved even though vortex limiter position is increased. It can be clearly seen that reverse flow cyclones are more efficient for separation processes according to axial flow cyclones (Figure 8). Particle collection efficiency of reverse flow cyclones are not changed significantly due to EOVS and induced vortex is effective in

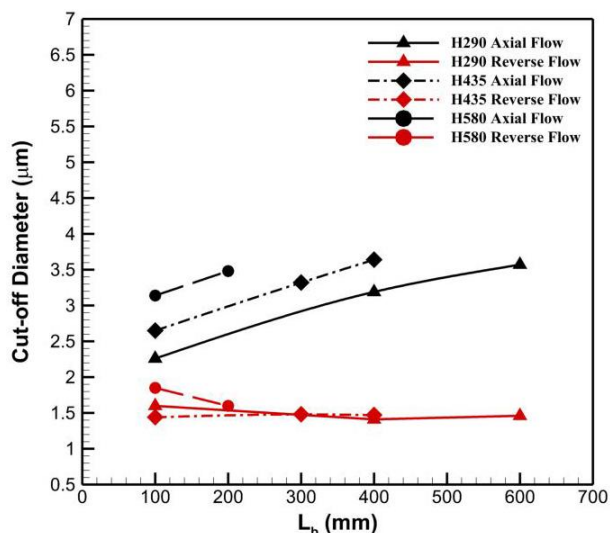


Figure 7. Collection efficiency of different geometric configurations for axial and reverse flow novel cyclones

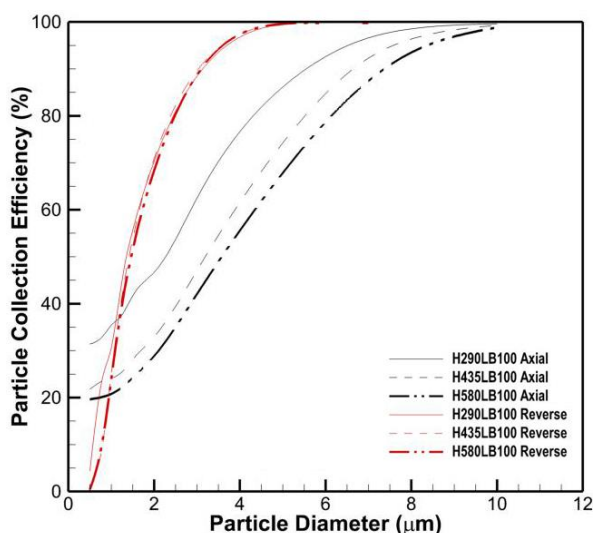


Figure 8. Grade efficiency curves of H290 for axial and reverse flow novel cyclones

separation space. For the other cyclones with EOVC give similar results. Collection efficiency of axial flow novel cyclone was decreased with increasing vortex limiter position (L_b).

4 Conclusions

Axial and reverse flow novel cyclones have been numerically analyzed using Reynolds Stress Model (RSM), in terms of collection efficiency and pressure drop. The following conclusions have been obtained.

- EOVC occurred for all geometric configurations of reverse flow cyclones.
- EOVC effects flow field and pressure drop. Cut-off diameters are similar due to inefficient separation

space below vortex end. Also primary vortex induces a secondary vortex probably due to precession of primary vortex. This is a type of fluid coupling [9].

- Generally, increasing H and L_b causes decreased pressure drop and increased cut-off diameter.
- Contrary to axial flow cyclone, reverse flow cyclone has greater pressure drop but more efficient in terms of particle separation.
- Comparison of the same configuration of axial and reverse flow cyclone geometries shows that; reverse flow cyclones provide higher pressure drop between 65 to 153%, and less cut-off diameter between 29 to 72% comparing to axial flow cyclones.

Acknowledgement

The authors gratefully acknowledge the financial assistance from the Scientific and Technological Research Council of Turkey (No. 114M591).

References

- [1] I. Karagoz, A. Avci "Modelling of the Pressure Drop in Tangential Inlet Cyclone Separators" *Aerosol Science and Technology* 39:9 (2005) 57-64. DOI:10.1016/j.jaerosci.2013.01.010
- [2] A. C. Stern, K. J. Caplan, P. D. Bush "Cyclone Dust Collectors" American Petroleum Institute, New York, 1955.
- [3] Y. Zhu, K. W. Lee "Experimental Study on Small Cyclones Operating at High Flowrates" *Journal of Aerosol Science* 30 (1999) 1303-1315. DOI:10.1016/S0021-8502(99)00024-5
- [4] I. Karagoz, A. Avci, A. Surmen, O. Sendogan "Design and Performance Evaluation of a New Cyclone Separator" *Journal of Aerosol Science* 59 (2013) 57-64. DOI:10.1016/j.jaerosci.2013.01.010
- [5] F. Tan, I. Karagoz, A. Avci "Effects of Geometrical Parameters on the Pressure Drop for a Modified Cyclone Separator" *Chemical Engineering Communications* 39:3 (2016) 576-581. DOI: 10.1002/ceat.201500182
- [6] J. Oh, S. Choi, J. Kim, S. Lee, G. Jin "Particle Separation with the Concept of Uniflow Cyclone" *Powder Technology* 254 (2014) 500-507. DOI:10.1016/j.powtec.2014.01.057
- [7] F. Kaya, I. Karagoz "Performance Analysis of Numerical Schemes in Swirling Turbulent Flows in Cyclones" *Current Science* 94 (2008) 1273-1278.
- [8] M. Sommerfeld "Theoretical and Experimental Modeling of Particulate Flow" Lecture Series 2000-6 (2000) von Karman Institute for Fluid Dynamics, Belgium.

- [9] A. C. Hoffmann, L. E. Stein "Gas cyclones and swirl tubes: Principle, Design and Operation" Springer, 2nd edition, 2008.
- [10] ANSYS, ANSYS Fluent 15.0 Theory Guide, Canonsburg, 2015.